Cell

A Temporal Chromatin Signature in Human Embryonic Stem Cells Identifies Regulators of Cardiac Development

Sharon L. Paige,[1,2,3,12] Sean Thomas,[9,12] Cristi L. Stoick-Cooper,[2,4,12] Hao Wang,[5,12] Lisa Maves,[10] Richard Sandstrom,[5] Lil Pabon,[1,2,3] Hans Reinecke,[1,2,3] Gabriel Pratt,[1,2,3] Gordon Keller,[11] Randall T. Moon,[2,5] John Stamatoyannopoulos,[5,6,*] and Charles E. Murry[1,2,3,7,8,*]

[1]Department of Pathology
[2]Institute for Stem Cell and Regenerative Medicine
[3]Center for Cardiovascular Biology
[4]Howard Hughes Medical Institute and Department of Pharmacology
[5]Department of Genome Sciences
[6]Department of Medicine
[7]Department of Bioengineering
[8]Department of Medicine/Cardiology
University of Washington, Seattle, WA 98109, USA
[9]Gladstone Institutes, San Francisco, CA 94158, USA
[10]Fred Hutchinson Cancer Research Center, Seattle, WA 98109, USA
[11]McEwen Centre for Regenerative Medicine, Ontario Cancer Institute, Toronto ON M5G 2C4, Canada
[12]These authors contributed equally to this work
*Correspondence: jstam@u.washington.edu (J.S.), murry@uw.edu (C.E.M.)
http://dx.doi.org/10.1016/j.cell.2012.08.027

SUMMARY

Directed differentiation of human embryonic stem cells (ESCs) into cardiovascular cells provides a model for studying molecular mechanisms of human cardiovascular development. Although it is known that chromatin modification patterns in ESCs differ markedly from those in lineage-committed progenitors and differentiated cells, the temporal dynamics of chromatin alterations during differentiation along a defined lineage have not been studied. We show that differentiation of human ESCs into cardiovascular cells is accompanied by programmed temporal alterations in chromatin structure that distinguish key regulators of cardiovascular development from other genes. We used this temporal chromatin signature to identify regulators of cardiac development, including the homeobox gene MEIS2. Using the zebrafish model, we demonstrate that MEIS2 is critical for proper heart tube formation and subsequent cardiac looping. Temporal chromatin signatures should be broadly applicable to other models of stem cell differentiation to identify regulators and provide key insights into major developmental decisions.

INTRODUCTION

Cardiovascular cells derived from pluripotent stem cells in vitro have potential both as a cell-based therapy for cardiac regeneration and as tools to analyze basic developmental processes (Murry and Keller, 2008). Insights from model organisms have permitted harnessing of the signaling pathways controlling cardiovascular development, enabling the directed differentiation of mouse and human embryonic stem cells (ESCs) into the major definitive cell types of the heart, namely cardiomyocytes, smooth muscle cells and endothelial cells (Bu et al., 2009; Domian et al., 2009; Kattman et al., 2006; Kattman et al., 2011; Laflamme et al., 2007; Murry and Keller, 2008; Yang et al., 2008). In contrast to the relatively advanced knowledge of signaling pathways, the epigenetic alterations that accompany or potentiate cardiogenesis are largely unexplored.

Methylation of lysine residues on the tail of histone H3 accompanies many major genomic functional processes (Guenther et al., 2007; Ringrose and Paro, 2004; Schuettengruber et al., 2007). H3K4me3 and H3K36me3 are deposited by Trithorax group proteins and mark chromatin associated with, respectively, transcription initiation and elongation (Bannister et al., 2005; Li et al., 2007; Vakoc et al., 2006). H3K27me3 modifications result from activities within the Polycomb repressive complex 2 (PRC2), which includes SUZ12 and EZH2 (Boyer et al., 2006; Lee et al., 2006; Simon and Kingston, 2009). Studies of the distribution of H3K27me3 in both mouse (Bernstein et al., 2006) and human (Hawkins et al., 2010; Pan et al., 2007) ESCs have revealed that H3K27me3 deposition is preferentially enriched at promoters of regulatory genes (Boyer et al., 2006; Lee et al., 2006) controlling diverse developmental pathways including neuronal (Mohn et al., 2008a) and hematopoietic lineages (Mazzarella et al., 2011a), where frequently, in combination with H3K4me3, it may denote "poising" of genes that are destined for rapid activation upon

lineage commitment (Bernstein et al., 2006; Rada-Iglesias and Wysocka, 2011). Indeed, "bivalent" promoters marked by both H3K4me3 and H3K27me3 in pluripotent cells are found to have either the H3K4me3 or the H3K27me3 mark (but not both) in definitive cell types, implying that this bivalency resolves to either a transcriptionally active or silent state (Mikkelsen et al., 2007). It is currently unknown how Polycomb- and Trithorax-related histone modification patterns evolve during the transition from pluripotency to definitive cells during lineage differentiation. Moreover, because Polycomb-driven marking of key regulatory genes in ESCs is not specific to any given lineage, it is currently not possible to identify lineage-specific regulators simply from the chromatin state of pluripotent stem cells.

We sought to determine whether temporal patterning of histone modifications during differentiation along a defined lineage would clarify the relationships among key regulators of lineage-specific differentiation and further distinguish regulatory from lineage-specific structural genes. Specifically, we hypothesized that key regulators of differentiation would show stage-specific changes in H3K4me3 and H3K27me3 because inappropriate activation or silencing of these genes could alter cell fate by affecting many downstream target genes. The differentiation of human ESCs into cardiomyocytes has been extensively described (Kattman et al., 2011; Laflamme et al., 2007; Yang et al., 2008) and is of great potential therapeutic importance (Murry and Keller, 2008). We therefore asked how chromatin modifications evolve temporally along the cardiac differentiation axis and whether the temporal patterning of histone modifications might provide a reliable signature that could discriminate key known regulators of cardiovascular development, as well as enable the identification of previously undiscovered regulators.

RESULTS

Directed Differentiation of Human ESCs into Cardiomyocytes

Directed differentiation of H7 human ESCs to the cardiovascular lineage was achieved by allowing the cells to form embryoid bodies (EBs) in the presence of defined serum-free medium as previously described (Kattman et al., 2011; Yang et al., 2008). Mesoderm induction was accomplished using bone morphogenetic protein 4 (BMP4), activin A and basic fibroblast growth factor (bFGF). On day 5 (T5) of differentiation, a tripotential cardiovascular progenitor emerges, identified based on low expression of VEGFR2 (KDR) and PDGFRα (Kattman et al., 2011). Over time, this progenitor gives rise to cultures that contain predominantly cardiomyocytes and also contain endothelial cells and smooth muscle cells, identified by flow cytometry for cardiac troponin T (cTnT), CD31/PECAM1, and smooth muscle alpha actin (SMA), respectively (Figure S1 available online). For all genome-wide experiments, parallel samples were maintained in culture after the times of harvest for immunoprecipitation, and only runs that were >80% KDR+/PDGFRα+ at the T5 progenitor stage and >50% cTnT+ cardiomyocytes at the T14 definitive cardiovascular cell stage were used.

Chromatin States Measured along the Time Course of Differentiation

We used chromatin immunoprecipitation coupled to massively parallel sequencing (ChIP-seq) to map H3K4me3, H3K27me3, and H3K36me3 modifications genome-wide at five key developmental stages during cardiovascular directed differentiation including pluripotent cells (T0), mesodermal progenitors (T2), specified tripotential cardiovascular progenitors (T5), committed cardiovascular cells (T9), and definitive cardiovascular cells (primarily cardiomyocytes, T14). We performed differentiation and ChIP-seq experiments in duplicate, with high reproducibility between biological replicates at each time point (average Pearson correlation 0.94). Figure S2A shows two biological replicates for chromatin modification at the *TBX5* locus, a transcription factor (TF) implicated in generation of the first heart field (Takeuchi et al., 2003). Across all time points, all three histone modification patterns with respect to the transcription start site (TSS) showed the expected morphologies (Figure S2B), with H3K4me3 signal peaking within a narrow window around the TSS, H3K27me3 signal peaking in the vicinity of the TSS (though more broadly distributed than H3K4me3) with a prominent decrease over the TSS (consistent with reduced nucleosomal density and increased turnover in this region [Möbius and Gerland, 2010]), and H3K36me3 signal increasing rapidly from the TSS region to a plateau over the gene body, consistent with its deposition by the elongating polymerase complex (Pjanic et al., 2011).

Identification of Distinct Chromatin Signatures for Different Functional Categories of Cardiac Factors

To gain insight into the pattern of sequential epigenetic alterations accompanying cardiovascular differentiation, we next examined the histone modification profiles and RNA expression of genes with established roles in heart development and function. These ranged from sequence-specific transcriptional regulators, such as *NKX2.5* (Figure 1A), to cardiomyocyte contractile proteins, including alpha myosin heavy chain (*MYH6*) (Figure 1B), as well as genes expressed in cardiovascular progenitors, smooth muscle cells and endothelial cells (Figures S3A–S3C). A majority of cardiac transcription factors showed high levels of H3K27me3 during pluripotency that gradually decreased as differentiation progresses, paralleled by gradual increases in H3K4me3, H3K36me3, and RNA expression (Figures 1A, 1C, and 1E). Similarly, many of the members of key signaling pathways involved in cardiac development, such as the TGFβ family, Wnt, Notch, Hedgehog, the FGF family, PDGF, and VEGF showed stage-specific activation (H3K4me3, H3K36me3, RNA expression) and repression (H3K27me3), compatible with tight control over signaling pathways that direct cell fate (Figure S3D). In contrast, although genes encoding cardiomyocyte contractile proteins showed similar time-dependent increases in H3K4me3, H3K36me3, and RNA expression, these genes did not have appreciable levels of H3K27me3 deposition at any time (Figures 1B, 1D, and 1F). As such, the temporal evolution of histone modifications provides a chromatin "signature" that differentiates key cardiac regulatory genes, including both transcription factors and soluble signals, from lineage-specific genes encoding proteins that regulate cardiac function and homeostasis.

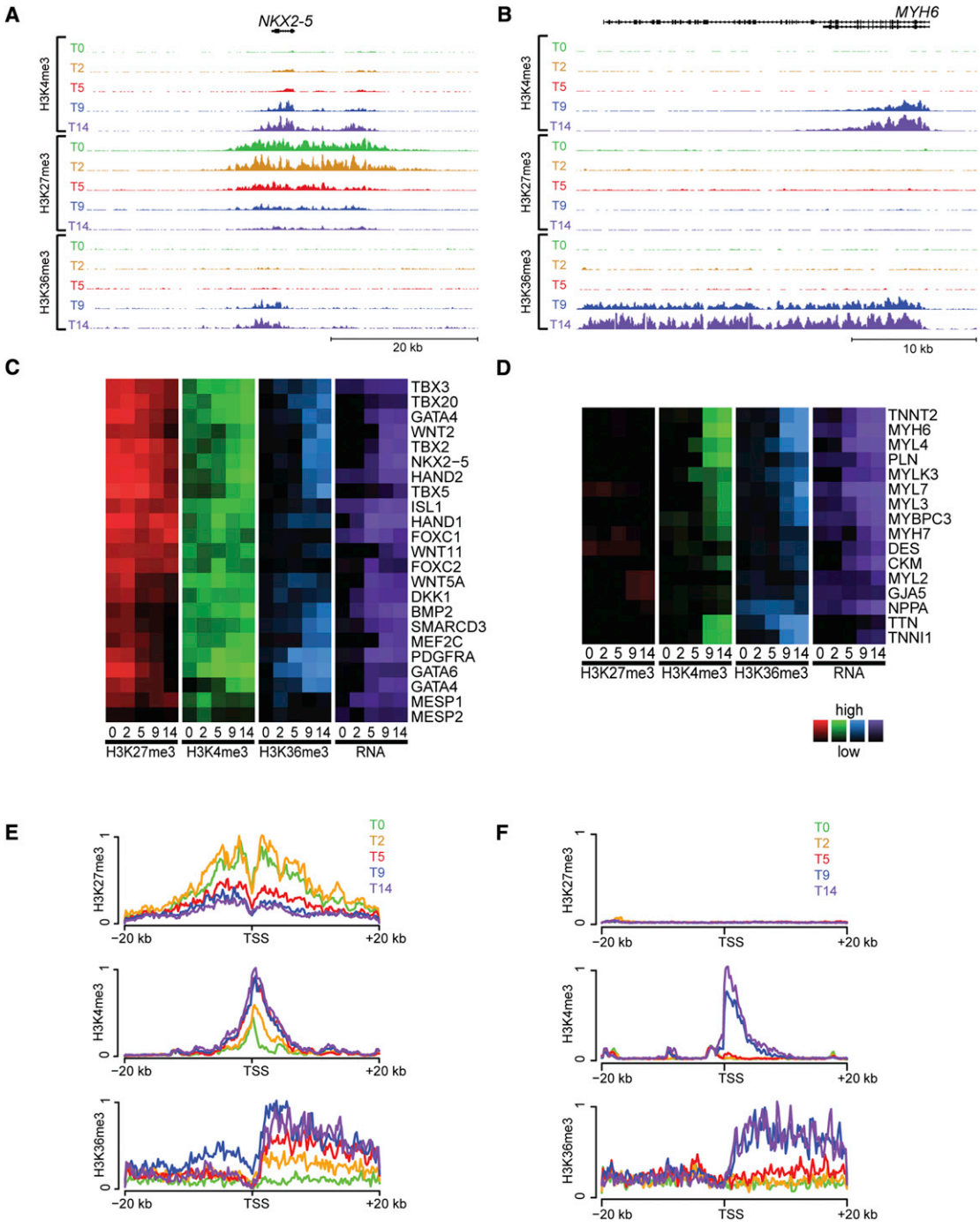

Figure 1. Key Regulators of Cardiac Differentiation Share a Temporal Chromatin Signature

(A–F) At five different time points of directed differentiation of human embryonic stem cells into cardiomyocytes (T0, 2, 5, 9, and 14), the levels of histone modifications H3K4me3 (activating), H3K27me3 (repressing) and H3K36me3 (transcribed) are shown within a ~50 kb region around (A) *NKX2-5*, a well-known regulator of cardiac differentiation (scales used: 1 to 250/150/50 tags per 150 bp for H3K4me3/H3K27me3/H3K36me3) and (B) *MYH6*, a well-known structural component of cardiac cells (scales used: 1 to 500/100/50 tags per 150 bp for H3K4me3/H3K27me3/H3K36me3). The relative levels of histone modifications (red, green and blue) and RNA expression (purple) are shown for (C) selected regulators of cardiac differentiation and (D) cardiac structural factors at all five time points. The averaged levels of epigenetic marks within ±20 kb of the TSS of (E) known regulators of cardiac differentiation and (F) known cardiac structural factors are plotted across all five time points (0, 2, 5, 9, 14 = green, yellow, red, blue, purple). For key regulators of cardiac differentiation, levels of H3K4me3 and H3K36me3 increase during differentiation while H3K27me3 begins high and decreases, while H3K27 remains consistently low for cardiac structural factors. Note *GATA4* is shown twice in panel (C) due to activation of two different promoters in our system. See Figure S3 for patterns found for other gene groups. See also Figures S1 and S2.

The Temporal Chromatin Signature of Cardiac Regulators

To assess the cardiac lineage-specificity of the temporal chromatin signature for cardiac regulators, we compared this signature with the temporal chromatin patterns at genes involved in specification of noncardiac mesoderm, neuroectoderm and endoderm fates (Figures S3E–S3I). Similar to cardiac transcription factors, most of the major transcription factor genes involved in hematopoiesis (e.g., *TAL1, RUNX1, HHEX* and *LMO2*) and skeletal muscle differentiation (e.g., *MYOD1, MYF5,* and *MYF6*) had low levels of H3K4me3 and high levels of H3K27me3 in the pluripotent state. However unlike cardiac TFs, noncardiac factors do not activate in this system and generally resolve to only H3K27me3 by T5. Some lineage-selective factors such as *GATA1*, a key regulator of erythroid fate, showed negligible levels of any of the histone modifications at any time point. Genes encoding transcription factors involved in neuroectoderm differentiation, such as *NEUROD1*, show high levels of H3K27me3 (often in large domains (Guenther et al., 2010)) in combination with low H3K4me3 in the pluripotent state (Figure S3H). But whereas H3K27me3 levels at neuroectodermal genes remain high throughout differentiation, they evince a dramatic drop in H3K4me3 by T2. Notably, hematopoietic and skeletal muscle transcription factors also show declines in H3K4me3 but not until T5. This ordering recapitulates the later fate choice for mesoderm subtypes versus the early choice of primary germ layer (mesoderm versus ectoderm). Interestingly, several genes typically associated with endoderm formation are activated at T5, including *FOXA2* and *SOX17.* This could be due to the presence of a small number of endodermal cells in our cultures or the fact that many of these genes have roles in both mesoderm and endoderm formation.

Identification of New Regulators of Human Cardiac Development

We next sought to determine if the temporal chromatin signature of cardiac regulators could be used to identify regulators of human cardiac development. Using a curated set of known cardiac regulators (Figure 1), we developed a classifier based on the concomitant induction of mRNA, loss of H3K27me3 marks, and anticorrelation coefficients of the H3K4me3 and H3K27me3 signals over the time course (see Experimental Methods). Next, we scored each gene against the classifier and rank-ordered each gene at T5, T9, and T14 by its classification score. For comparison, we performed a similar ranking using a classifier based on mRNA expression only. Figure 2A shows the top ten genes at each time point using each algorithm, functionally annotated as cardiac developmental regulators, cardiac structural genes, developmental regulators with unknown cardiac roles, and all other genes (including unknown cardiac or developmental roles). A list of the top 100 genes identified by using expression alone and chromatin + expression at each time point is shown in Figure S4. Using mRNA expression alone, 14 nonredundant genes comprised the top 10 list at the three time points. Of these, six (43%) encoded cardiac structural proteins, five (36%) encoded known cardiac developmental regulators, one (7%) encoded a developmental regulator with unknown cardiac function, and two (14%) were genes with unknown function. Using the chromatin + expression method, the top ten lists across all time points contained 15 nonredundant genes. In contrast to the mRNA expression-only approach, 11 of these genes (73%) encode developmental regulators with known cardiac roles, three others (20%) encode developmental regulators with unknown cardiac roles, and one gene (7%) encodes a protein of unknown function. Interestingly, this gene (*CCDC92*) is predicted to contain a coiled-coil domain, which is found in many transcription factors. Notably, none of the top-scoring genes in the combined algorithm encode cardiac structural proteins.

Beyond the top 10, the chromatin + expression algorithm identified many genes with less well-defined roles in cardiac development including transcription factors, cell surface proteins, signaling ligands, extracellular matrix proteins, and enzymes. Gene ontology analysis demonstrated that the top 100 genes identified by using chromatin + expression are highly enriched for regulation of transcription and differentiation functions (Figure 2B). To determine the accuracy with which each classifier could discriminate known cardiac regulators from all other genes, and specifically from cardiac structural genes, we computed a receiver operating characteristic (ROC) curve for each class using both the mRNA expression-only and the chromatin + expression classifier. These showed that the combined (histone modification + expression) classifier had extremely high sensitivity and specificity both for discrimination of cardiac regulators from all genes (ROC = 0.994) and from cardiac structural proteins (ROC = 1.000) (Figure 2C). By contrast, a classifier based on temporal mRNA patterns alone can reasonably discriminate genes with a cardiac role from all other genes but cannot distinguish regulators from cardiomyocyte structural proteins involved in muscle contraction and energy production.

Analysis of Temporal Chromatin Dynamics Identifies Regulators of Other Cellular Fates

The selective discrimination of genes regulating cardiac differentiation by comparison of epigenetic profiles and expression led us to ask whether we could identify factors not expressed during the cardiovascular differentiation process that regulate other lineage fates. To explore this, we first examined a curated list of neuroectodermal regulatory genes and structurally-related genes. Remarkably, these showed distinct temporal chromatin signatures for developmental regulators versus structural gene classes, even though the constituent genes were not significantly expressed at any time in our cardiac directed differentiation system (Figures 3A–3F).

To systematically identify candidate regulators of other cellular fates, we performed principal component analysis of the chromatin modification profiles (see Experimental Procedures). This analysis revealed that genes with similar roles in cell fate determination clustered together (Figure 3G), remaining distinct from other lineage-specific genes. This result suggests that a rich layer of information on developmental programming can be mined from temporal analysis even of a single lineage, which may in turn provide insight into the mechanisms that determine numerous cell fates.

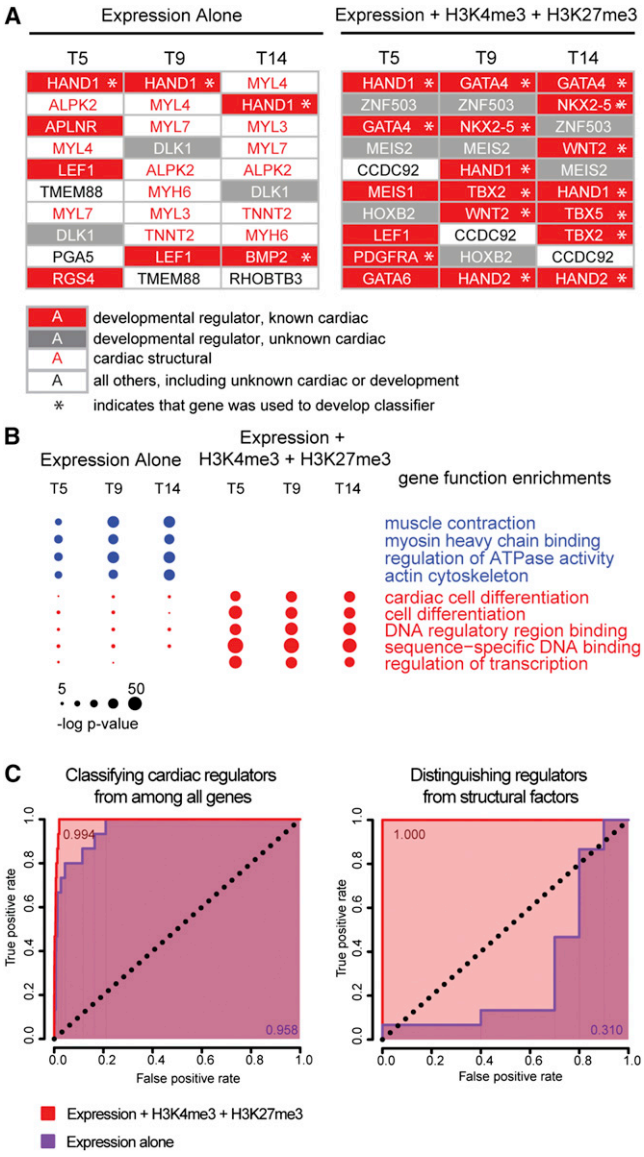

Figure 2. Accurate Discrimination of Key Regulators of Cardiac Differentiation from Other Lineage-Specific Genes

(A) All genes were ranked by two different methods in order to identify key regulators of cardiac differentiation. They were ranked at days 5, 9, and 14 by a formula using either (left) RNA expression alone, or (right) one that accounts for levels of H3K4me3, H3K27me3 and RNA expression. At each time point the top 10 candidate regulators are depicted for the respective methods. Developmental regulators with known roles in cardiac differentiation are shown in white text on red background, developmental regulators with no currently appreciated role in cardiac differentiation are shown in white text on gray background, and genes whose function pertains to the structure and function of heart cells with no known regulatory roles are shown in red text on white background. All other genes are shown in black text on white background. Genes that were used in the training set for identifying the chromatin + expression regulator signature are indicated with an asterisk.

(B) The top 100 candidates provided by each ranked list (see Figure S4) were analyzed to determine the degree to which the lists were enriched in 11 key gene ontology functional categories. The size of each circle is proportional to the significance of the enrichment of genes with the indicated functional role within the given list of 100 genes at each time point/method of ranking genes. Ranking genes using H3K4m3, H3K27me3 and RNA expression yields lists that are not contaminated by structural factors and are more enriched with known regulators of cardiac differentiation.

(C) Classification based on H3K4me3, H3K27me3 and expression (red) is more specific and sensitive than classification based on expression alone (purple). Shown are ROC curves for the identification of key regulators of cardiac differentiation from among all genes (left) or among all genes involved in heart development (right). The expression-only classifier systematically misclassifies structural factors that are involved in heart function but do not regulate cardiac development (right), leading to a lower area under the curve when classifying key regulators from among all genes (left). The genes used to generate true-positives for cardiac regulatory and structural genes are given in Figure 1. See also Figure S4.

Functional Validation of Chromatin Dynamics-Based Predictions

We next sought to confirm whether the temporal chromatin signature of cardiac regulators could identify bona fide cardiac regulators. Among the genes we identified without known roles in cardiac development was the homeodomain-containing transcription factor *MEIS2* (Figure 4). MEIS transcription factors interact with HOX and PBX transcription factors to regulate downstream targets in multiple cellular processes, and previous studies have demonstrated a requirement for the related gene, *Meis1*, in mouse and zebrafish heart development (Maves et al., 2009; Minehata et al., 2008; Stankunas et al., 2008). As shown in Figure 4A, *MEIS2* shares the histone modification pattern we have identified as a marker of cardiac regulatory genes. In zebrafish there are two orthologs of *MEIS2*: *meis2a* and *meis2b*. Interestingly, in situ time course experiments carried out in developing zebrafish embryos shows *meis2b* expression in the heart field closely resembles that of *gata4*, a known cardiac transcription factor (Figures 4B and 4C). In addition, *meis2b* expression is observed in the developing hindbrain and somites as previously described (Zerucha and Prince, 2001).

To validate the predicted role of *MEIS2* in cardiac development based on its temporal chromatin signature, we utilized antisense morpholino oligonucleotide (MO) knockdown in developing zebrafish embryos (Figure 5). We found that delivery of a splice-blocking MO directed against *meis2b* ("*meis2b*-MO") into fertilized zebrafish eggs results in defective cardiac morphogenesis. Defects are evident as early as 19 hr postfertilization (hpf), when *meis2b*-MO embryos fail to fuse their bilateral heart fields into a linear heart tube at the midline (Figure 5A) (Glickman and Yelon, 2002). At 24 hpf, heart tubes have formed in *meis2b*-MO embryos, but they demonstrate an early looping defect as evidenced by the midline to right-sided location of the developing linear heart tube compared to the left-sided developing heart in control-MO embryos (Figure 5A) (Glickman and Yelon, 2002). By 48 and 72 hpf, control-MO embryos have normally looped hearts (Glickman and Yelon, 2002), while the *meis2b*-MO embryo hearts remain linear, displaying a persistent looping defect (Figures 5A and 5B). Furthermore, *meis2b*-MO embryos have a markedly reduced heart rate at 72 hpf (92 ± 10 beats per minute) compared with control-MO embryos (154 ± 16 beats per minute), and they have pericardial edema indicative of cardiac failure (Figures 5C and S5). These findings indicate a requirement of *meis2b* for normal heart function (Figure 5D). Of note, these phenotypes are not attributable to a general

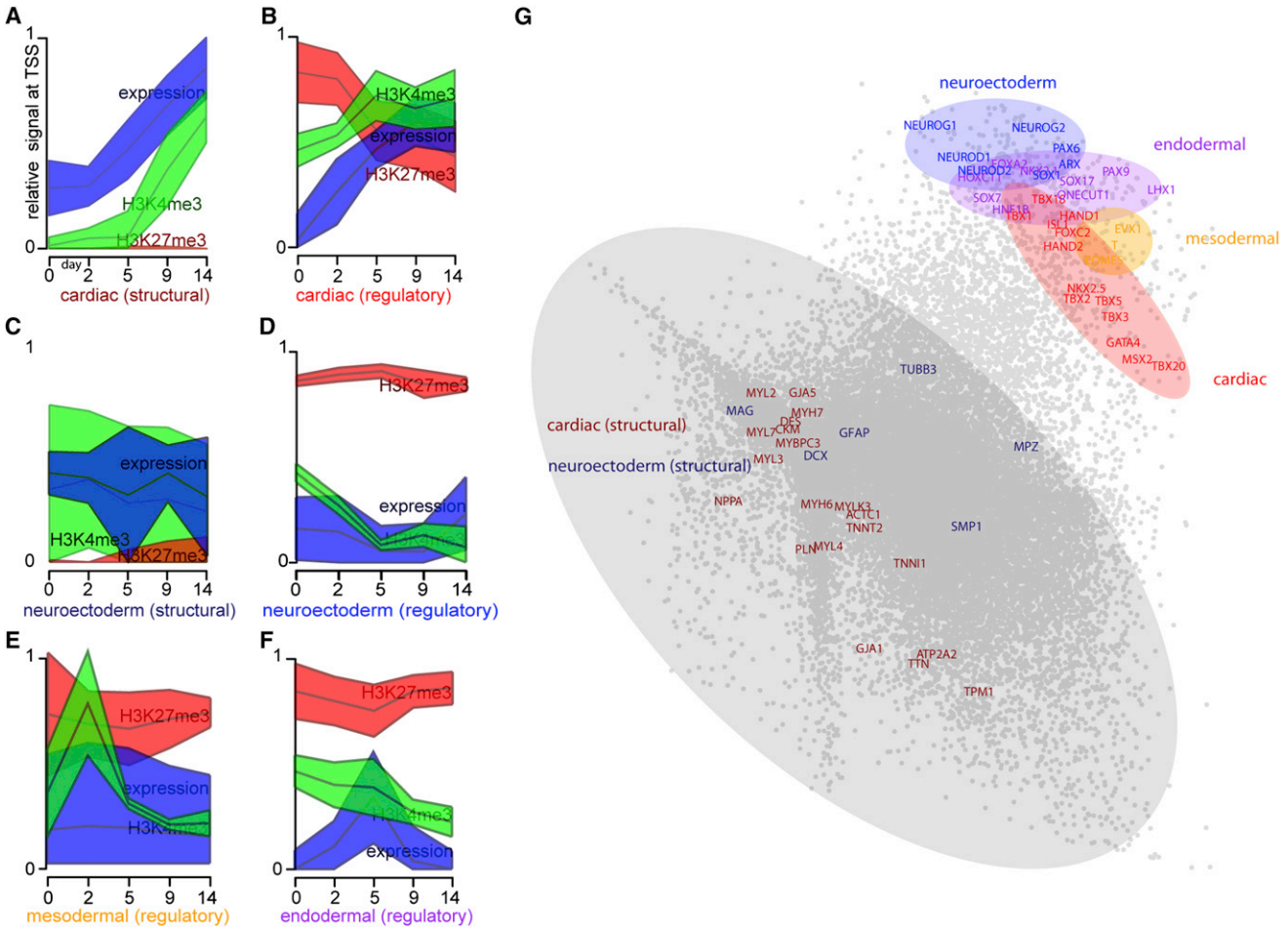

Figure 3. Temporal Chromatin Signatures Enable Cross-Lineage Identification of Key Regulatory Factors

(A–F) The median levels (middle line) and 95% confidence intervals (shaded regions) of H3K27me3 (red), H3K4me3 (green), and RNA expression (blue) at each time point are depicted for several categories of genes: (A) genes involved in cardiac structure and function, (C) genes involved in neuroectoderm structure/function, and regulators of differentiation for (B) cardiac, (D) neuroectoderm, (E) mesoodermal and (F) endodermal cells. (A–F) were identically normalized, such that the lowest and highest values for each individual mark across all time points and gene groups were plotted as 0 and 1, respectively.

(G) Using principle component analysis, the 15 dimensional data for each gene (five time points * three measurements of chromatin and mRNA) were reduced to two dimensions, and a scatterplot is shown depicted the relative locations of each gene in the reduced-dimensional space. Genes involved in structure and function of cells are contained within the largest cluster (gray) distinct from the cluster containing key regulators of cellular fate: cardiac (red), neuroectoderm (blue), endoderm (purple), and mesoderm (yellow). Nonannotated genes within each of the colored domains have a high probability of having unappreciated roles as key regulators of cellular fate.

developmental delay upon knockdown of *meis2b* as embryos were compared based on number of somites (developmental stage) as well as time postfertilization. These phenotypes are also unlikely to be attributable to off-target effects because a separate, translation-blocking *meis2b* morpholino produces similar looping defects (Figure S5 and data not shown). These data establish *meis2b* as a regulator of cardiac development, confirming the chromatin signature-based prediction.

DISCUSSION

The chromatin landscape of both mouse and human ESCs has been intensively investigated. In the pluripotent state, many developmental loci are marked with both activating H3K4me3 and repressing H3K27me3 and are thus termed ''bivalent'' (Azuara et al., 2006; Bernstein et al., 2006; Pan et al., 2007). The notion is that these genes are simultaneously suppressed but poised for activation should the cell receive appropriate cues. Bivalent promoters have also been found at developmental loci in mouse embryos, both in the inner cell mass and trophectoderm, and also in zebrafish embryos (Dahl et al., 2010; Lindeman et al., 2010; Vastenhouw et al., 2010). Other studies have shown that bivalent promoters are present in progenitor and adult stem cell populations, including neural progenitors, mesenchymal stem cells, and hematopoietic stem cells, and that these ultimately resolve to either active or inactive upon differentiation (Collas, 2010; Cui et al., 2009; Mazzarella et al., 2011b; Mohn et al., 2008b).

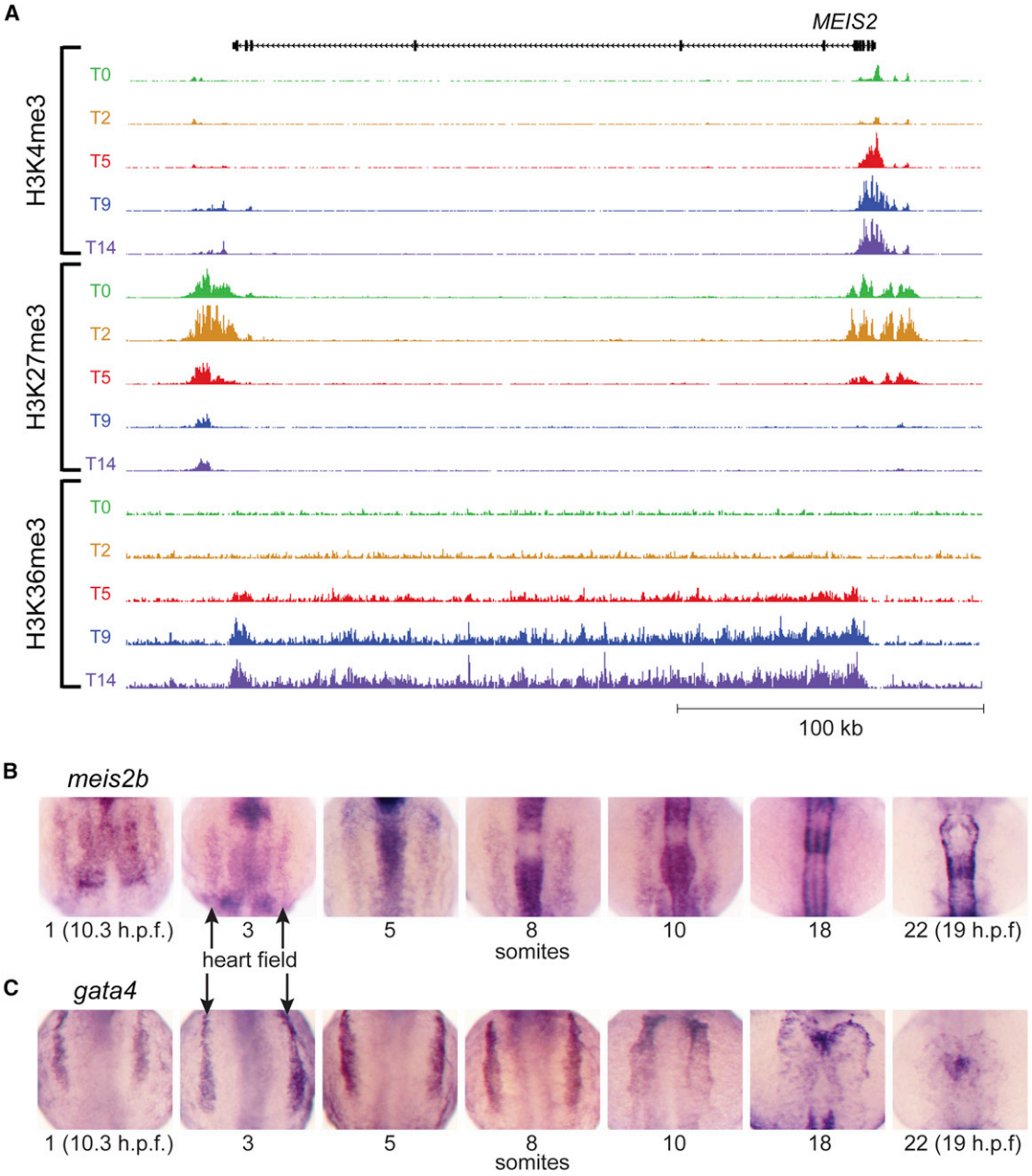

Figure 4. *MEIS2* Chromatin Modifications during hESC Differentiation and Expression in Developing Zebrafish Embryos Resembles Other Regulators of Cardiac Development

(A) The temporal pattern of epigenetic marks at the *MEIS2* locus is similar to that of other regulators of cardiac development shown in Figure 1 (scales used: 1 to 250/150/25 tags per 150 bp for H3K4me3/H3K27me3/H3K36me3).

(B) Zebrafish *meis2b* expression are shown for developing embryos at the 1, 3, 5, 8, 10, 18, and 22 somite stages, showing (C) similar expression patterns within the bilateral heart fields (arrows) to *gata4* through the 10 somite stage. By 18 somites, *meis2b* is no longer expressed in the cardiac mesoderm whereas *gata4* maintains expression.

We sought to characterize the epigenetic changes that occur during cardiovascular differentiation from human ESCs by performing genome-wide mapping of three histone modifications, H3K4me3, H3K27me3, and H3K36me3, at five key developmental time points. Our study shows that the temporal trajectories of H3K4me3 and H3K27me3 during differentiation are more complex than a simple ''resolution from bivalency'' model. As an example of this, *FGF19* and *NODAL* are highly transcribed in human ESCs with high levels of H3K4me3 and low levels of H3K27me3 (Figure S3D). They subsequently lose H3K4me3 and gain H3K27me3 over time. If one were only to have taken time points T3 (sometime between T2 and T5) and T14, one

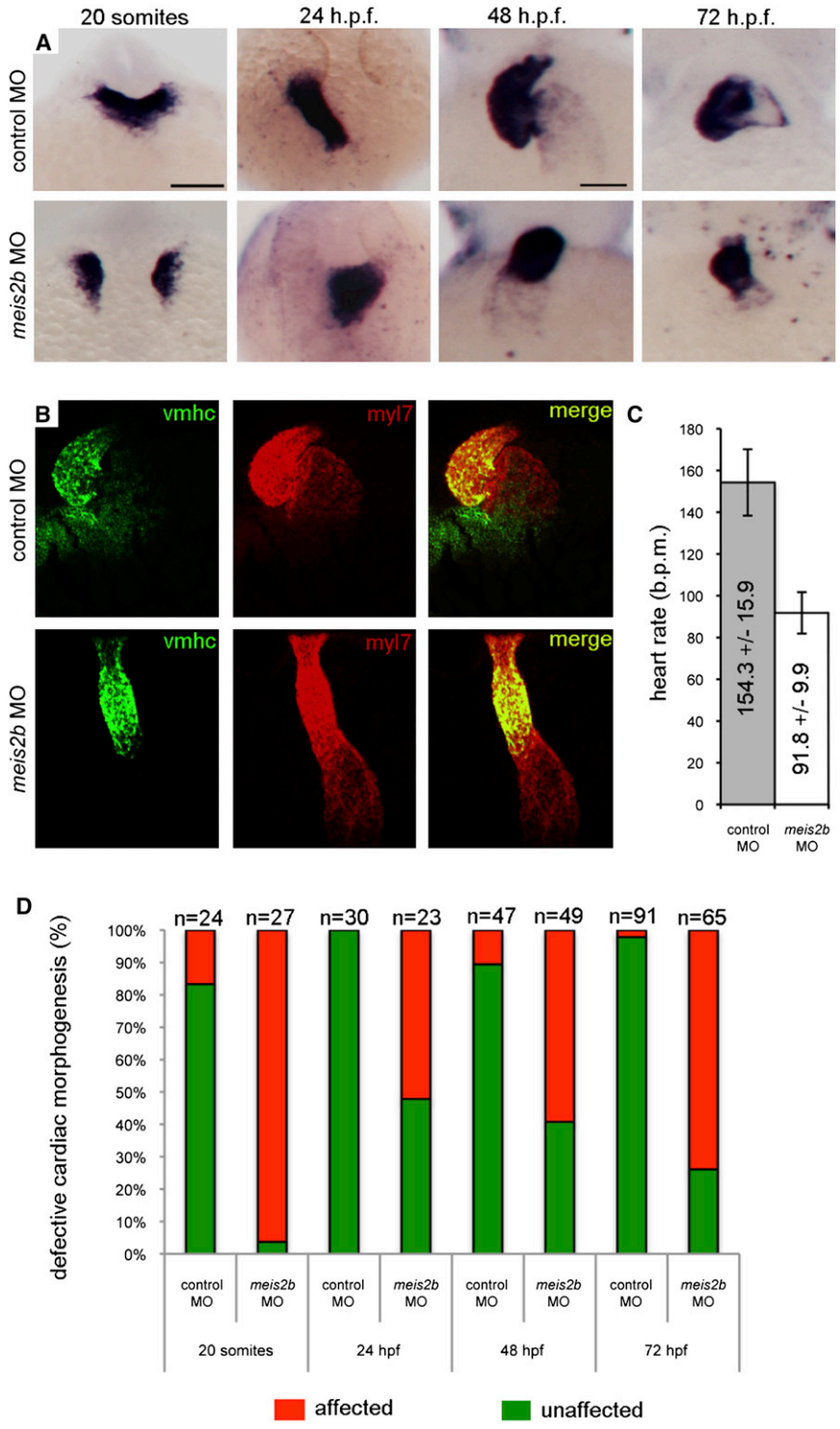

Figure 5. *meis2b* Is Required for Cardiac Morphogenesis

(A) Expression of *myl7* at 19 hpf, 24 hpf, 48 hpf, and 72 hpf in control-MO (top row) versus *meis2b*-MO (bottom row) injected zebrafish embryos. Dorsal view, anterior is up in 20 somite and 24 hpf embryos. Ventral view, anterior up in 48 hpf and 72 hpf embryos. At 19 hpf, *meis2b*-MO injected embryos display defects in fusion of the *myl7*+ cardiac progenitors at the midline compared with control-MO injected embryos. By 24 hpf, the heart tube has formed in *meis2b* morphants but displays aberrant cardiac morphogenesis and is either sitting at the midline or moving down the right side of the embryo, compared with the control-MO injected embryos where normal heart development proceeds with the heart tube emerging from under the head, down the left side of the embryo. At 48 and 72 hpf, control MO injected embryos display normal cardiac looping, whereas *meis2b*-MO injected embryos' hearts have not looped.

(B) This failure of cardiac looping in *meis2b*-MO injected embryos is further evident in *vmhc* (green) and *myl7* (red) double fluorescent in situs at 48 hpf.

(C) Heart rate is significantly reduced in *meis2b*-MO injected embryos compared with control-MO injected embryos at 72 hpf (b.p.m. = beats per minute) Mean heart rate ± SD is shown, n = 10. $p = 4 \times 10^{-9}$ (Student's t test, two-tailed).

(D) Percentages of embryos displaying the depicted phenotypes.

Scale bars, (A, top left), 100 μm, and (A, top third from the left), 50 μm. See also Figure S5.

might conclude that the genes began in a bivalent state and then resolved toward repression, whereas in reality the "bivalent" appearance was merely an artifact of the complete reversal from H3K4me3 to H3K27me3. Yet another example is the set of genes involved in mesodermal differentiation (Figure S3E), which are highly expressed despite being heavily marked with H3K27me3. These and other examples point to a complex regulatory relationship than cannot be described by a simple "resolution from bivalency" model.

Transcription factors and signaling molecules known to play critical roles in cardiovascular development, such as *NKX2.5,* showed a unique chromatin signature that consisted of high enrichment for H3K27me3 in pluripotent ESCs that gradually decreased as H3K4me3, H3K36me3, and RNA expression increased over time. In contrast, structural proteins like alpha-myosin heavy chain *(MYH6)* demonstrated markedly increased H3K4me3 enrichment and RNA expression at later time points, without early H3K27me3 repression. The differences in chromatin markings between genes encoding developmental regulators and structural proteins are consistent with previous studies comparing pluripotent and differentiated cells. Our study shows further that the complex temporal chromatin patterns over a time course of differentiation contain a far richer amount of

information regarding the exact function of the genes they are marking.

To use the information contained within the temporal chromatin signatures to identify regulators, we developed a classifier to rank genes according to the likelihood that a given gene would modulate cardiogenesis. Interestingly, several genes that ranked highly were transcription factors that had not been previously studied in cardiac development. We therefore tested our hypothesis that these genes were in fact previously unappreciated key regulators of heart development by utilizing morpholino knockdown technology in zebrafish embryos. Indeed, knockdown of *meis2b* resulted in severe defects in heart looping in early stage zebrafish embryos. This provides in vivo evidence that our methodology of coupling stem cell differentiation with histone modification pattern identification can identify regulators of development. It is worth noting that several of these regulators could be identified using the rank list of the top 100 genes based on expression alone (Figure S4). However, these regulators usually rank much lower down the list and could easily get lost amidst the noise of so many structural genes. For example, *MEIS2* ranked 4^{th} at T5, 4^{th} at T9, and 5^{th} at T14 using the chromatin signature ranking but 49^{th} at T5, 37^{th} at T9, and 48^{th} at T14 based on expression alone. Our data set will thus serve as a resource for scientists and clinicians across multiple fields. The list of cardiac regulators is extensive and each potential candidate gene warrants further investigation to flesh out its role in differentiation and/or morphogenesis. One can imagine that perturbations of these regulators could alter cardiogenesis during human development. Thus, screening for genetic etiologies of congenital heart disease could be expanded to include our list of regulators.

It is interesting to consider why the chromatin dynamics of genes involved in developmental regulation are so different from structural genes that regulate the function of differentiated cells. The principal difference in chromatin signatures is the high degree to which developmental regulators are repressed by H3K27me3 prior to their expression, whereas structural genes show no such modification. We propose that the consequence of inappropriate activation of developmental regulators is more deleterious, e.g., by inducing the wrong cell type, proliferative state, or survival/death signals. These genes therefore require both loss of repression and gain of activation to be expressed. Conversely, inappropriate activation of a gene encoding contractile proteins, ion channels, or metabolic enzymes may have less severe consequences for development, and chromatin regulation through activation mechanisms achieves sufficient fidelity.

The establishment of human ESC technology opened the doors to analyses that can provide insights into human development that have not been possible before. Directed differentiation of human ESCs into numerous cell types has been one of the major advances in the field over the past 10 years. In addition to the cardiovascular directed-differentiation model system we utilized in this study, similar protocols exist for the generation of other cell types that are particularly relevant to regenerative medicine, including neurons (Lee et al., 2007) and pancreatic beta-cells (Phillips et al., 2007). Thus, our approach of mapping chromatin states over the course of differentiation could easily be applied to other cell lineages, thereby facilitating the identification of regulators of differentiation and development of other organ systems.

Several limitations of the approach used in this study are important to note. First, although the directed differentiation model is very robust, it is not perfect. We are able to obtain highly enriched populations of cardiovascular cells; however, noncardiac cells are also present in our cultures. Therefore, we cannot exclude the possibility that some of our chromatin patterns might be due to the presence of other cell types, such as noncardiac mesoderm and endoderm. That said, the cell populations analyzed in this study contained at least 80% progenitors at T5 and 50% cardiomyocytes at T14, so the majority of the chromatin patterns are likely informative for cardiac development. Another issue is that the efficiency of directed differentiation is often dependent on the particular ESC cell line used or even the batch of such cells used. Thus, it will be critical for these experiments to be repeated in other cell lines beyond the H7 ESC line used in our laboratory. Lastly, although human ESCs provide a platform to model human development in vitro, it is presently unclear how well this differentiation system mimics in vivo development in terms of expression patterns and epigenetic changes, such as histone modifications. These limitations are common to many directed differentiation systems, and reflect the current standard issues shared by stem cell biologists worldwide. On the other hand, there are currently no other ways to study early events in human development, and we were able to utilize our cardiovascular directed-differentiation system to identify regulators of heart development. Additionally, our study showed that the temporal chromatin profiles along cardiomyocyte differentiation contained enough information to identify genes with likely unappreciated roles in neurectodermal development, even though the vast majority of cells in the population split from that cellular-fate quite early in differentiation. As the chromatin states along other differentiation pathways are measured, the information from all of these model systems can be integrated using methods similar to those described in this study to provide even richer insights into all branches of developmental regulation.

EXPERIMENTAL PROCEDURES

Maintenance of Human Embryonic Stem Cells

H7 human ESCs were maintained on mouse embryonic fibroblasts (MEFs) in medium consisting of DMEM/F12 supplemented with 20% KnockOut serum replacement (Invitrogen), L-glutamine, nonessential amino acids, beta-mercaptoethanol, and 8 ng/ml basic fibroblast growth factor (bFGF, Peprotech). Cells were passaged by using collagenase IV and trypsin, as well as the ROCK inhibitor Y-27632 (10 μM, Tocris) to enhance cell survival. Prior to directed differentiation, human ESCs were passaged at least twice on Matrigel-coated plates to deplete the cultures of MEFs. For growth on Matrigel, cells were maintained in MEF conditioned medium (MEF-CM) supplemented with 8 ng/ml bFGF.

Cardiovascular Directed Differentiation

H7 human ESCs on Matrigel-coated plates were harvested by using Collagenase IV and trypsin as during passaging. For embryoid body formation, cells were gently broken up into clusters of roughly 25–50 cells and plated into low-attachment plates in StemPro-34 medium (Invitrogen) supplemented with L-glutamine, ascorbic acid, transferrin, and monothioglycerol (hereafter

referred to as StemPro backbone) plus 0.5 ng/ml bone morphogenic protein 4 (BMP4, R+D). After 24 hr, embryoid bodies were gravity-settled and replated in fresh StemPro backbone plus 10 ng/ml BMP4, 6 ng/ml Activin A (R+D), and 5 ng/ml bFGF. After 3 days, the embryoid bodies were dissociated into single cells using trypsin and seeded onto Matrigel-coated plates at a density of 5×10^5 to 1×10^6 cells/cm^2 in StemPro backbone. Medium was changed every 3–4 days thereafter until day 14 of differentiation.

Flow Cytometry

Cells were analyzed by flow cytometry at the cardiovascular progenitor (T5) and definitive cardiovascular cell (T14) stages of differentiation. Cultures were dissociated into single cells using trypsin enzymatic digestion. Progenitor stage cells were stained with mouse anti-human VEGFR2/KDR-PE (R+D) and mouse anti-human PDGFRα-APC (R+D). For intracellular staining, cells were fixed in 4% paraformaldehyde for 10 min followed by permeabilization with 0.75% saponin. Cardiomyocytes and smooth muscle cells were identified by staining with mouse anti-cardiac troponin T (LabVision/Neomarkers) and rabbit anti-smooth muscle actin (Abcam), followed by goat anti-mouse-PE (Jackson) and donkey anti-rabbit-APC (Jackson). Endothelial cells were identified using mouse anti-human CD31-PerCP-eFlour710 (eBioscience). Flow cytometric analysis was performed using a BD FACS Canto II machine.

Chromatin Immunoprecipitation Followed by Massive Parallel Sequencing

H7 human ESCs at different cardiovascular stages were crosslinked with 1% formaldehyde (Sigma) and sheared by Diagenode bioruptor. The antibodies used in ChIP assays were 9751 for histone H3 tri-methyl lysine 4 (Cell Signaling), 07-449 for histone H3 tri-methyl lysine 27 (Millipore), and ab9050 for histone H3 tri-methyl lysine 36 (Abcam). For each IP, Dynabeads (M-280, sheep anti-rabbit IgG, Invitrogen) were incubated with antibodies for 6 hr at 4°C and then incubated overnight with ~100 μg sheared chromatin. The complexes were rinsed sequentially with IP wash buffer I (50 mMTris-HCl pH 8.0, 150 mM NaCl, 1 mM EDTA [pH8.0], 0.1% SDS, 1% Triton X-100, 0.1% sodium deoxycholate), high salt buffer (50 mMTris-HCl pH8.0, 0.5 M NaCl, 1 mM EDTA [pH8.0], 0.1% SDS, 1% Triton X-100, 0.1% sodium deoxycholate), IP wash buffer II (50 mMTris-HCl [pH8.0], 1 mM EDTA pH8.0, 1% NP-40, 0.7% sodium deoxycholate, 0.5 M LiCl), and TE buffer (10 mMTris-HCl [pH8.0], 1 mM EDTA pH8.0). The complexes were incubated with elution buffer (10 mMTris-HCl [pH 8.0], 0.3 M NaCl, 5 mM EDTA [pH8.0], 0.5% SDS) supplemented with RNase A (Ambion) at 65°C overnight. After separation, the DNA was treated with Proteinase K and purified by PCR purification column (QIAGEN). The sequencing libraries were prepared following a standard protocol using PE adapters (Illumina). For each library, an Illumina Genome Analyzer was used to generate 36 base pair sequence reads, yielding an average of ~18 million tags that mapped uniquely to the human genome (hg18).

Affymetrix RNA Expression Array

At the five time points indicated, an aliquot of cells were harvested in RNAlater (Ambion) and stored at −20°C. Total RNA was isolated using RNeasy kits (QIAGEN) according to the manufacturer's instructions followed by quantification and quality assessment using a Bioanalyzer (Agilent). Approximately 3 μg RNA was subjected to in vitro transcription and labeling followed by hybridization to Affymetrix Human Exon 1.0 ST arrays (Affymetrix) according to the manufacturer's protocols.

Data Analysis

ChIP-seq tag density, the number of uniquely mapping sequenced tags within ± 75 bp, was calculated in 20 bp bins across the (hg18) reference human genome. Using annotated transcription start sites, the ChIP densities for three chromatin modifications (H3K4me3, H3K27me3, and H3K36me3) within 20 kb of each transcription start sites were collected at 20 bp resolution.

To determine the temporal chromatin profiles for different classes of genes TSS-centered profiles of chromatin changes were assembled. For H3K27me3 and H3K4me3 data, this was accomplished by "folding" the data within 2 kb of each TSS in half and performing a linear regression. The slope and intercept of the resulting line were directly proportional to the intensity of those signals and were used to assign a single number to each gene at each time point. For H3K36me3, the average signal intensity over the gene body was used as the signal intensity measure.

Two methods were used to rank genes according to potential roles as regulators of cardiac differentiation. The formulas for ranking genes according to these measures follow:

$$a_i = \sum_{j=1}^{n} x_{(i,j)} \cdot \left(x_{(i,t)} - \min\left(x_{(i,)}\right)\right)$$

$$b_i = a_i \cdot - \rho_{k4,k27} \cdot \sum_{j=1}^{n} k27_{(i,j)} \cdot \left(k4_{(i,t)} - \min\left(k4_{(i,)}\right)\right)$$

where "a" is the measure based on expression alone, and b is the measure based on expression (x), H3K4me3 (k4), and H3K27me3 (k27). The measure was calculated for each gene (i), using data from each of n = 5 time points (j), and also using information specific to a given time point of interest "t." The function "ρ" is the Pearson product moment correlation, and "min()" yields the minimum value from a set of numbers.

Principal component analysis was performed in R using 20 data points per gene, including five time points for each of four measurement types: H3K4me3, H3K27me3, H3K36me3, and RNA expression. The overview for all genes was plotted in 2D space according to the top three principal components.

Zebrafish Morpholino Injections and In Situ Hybridization

The strain Tg(acta1a:GFP) (Higashijima et al., 1997) was used as a wild-type zebrafish strain and was maintained, crossed, injected, raised, and staged as described (James et al., 2009) and in accordance with IACUC approved procedures. Heart rate was assessed in ten randomly selected embryos from each group (control-MO versus *meis2b*-MO) by visualizing the heart beat in living embryos and counting for 1 min. *myl7* and *vmhc* probes were synthesized from published constructs (Yelon et al., 1999). Stock morpholinos (MO; Genetools, Philomath, OR) were dissolved in ddH_2O to a concentration of 30 ng/nl, diluted to injection strengths (10 ng/nl for splice blocking E3I3 *meis2b*-MO [injected 4nl of 2.5ng/nl solution], 6 ng/nl for ATG blocking *meis2b*-MO], and 5 ng/nl (1–2 nl injected) Standard control-MO and injected into one-cell stage zebrafish embryos. The sequences for the morpholinos are as follows: Splice-blocking E3I3 *meis2b*-MO: ACCGAAATCAATAA CTTGCCTGTTT; ATG blocking *meis2b*-MO: 5′-CTTCGTACCGTTGAGCCATC AGCAT; Standard control-MO: 5′-CCTCTTACCTCAGTTACAATTTATA.

RNA in situ hybridizations were performed as previously described (Maves et al., 2009; Talbot et al., 2010). Phenotype was scored "affected" if the heart displayed a defect as pictured versus "unaffected" if the heart appeared normal, compared with controls.

ACCESSION NUMBERS

The GEO accession numbers for epigenetics data and for the expression data are GSE35583 and GSE19090, respectlively.

SUPPLEMENTAL INFORMATION

Supplemental Information includes five figures and can be found with this article online at http://dx.doi.org/10.1016/j.cell.2012.08.027.

ACKNOWLEDGMENTS

The authors thank Nina Tan, Mark Saiget, James Fugate, Kristen Lee, Rajinder Kaul, and Stanley Kim for technical expertise. This work was supported by NIH grants P01 GM081719, U01 HL100405, P01 HL094374, R01 HL084642, R01 HL64387, R03 AR057477, and UW ENCODE Center (U54HG004592). S.P. was supported through NIH F30 HL095343. H.W. was supported by R90HG004152. R.T.M. is an investigator of the HHMI.

Received: April 3, 2012
Revised: June 26, 2012
Accepted: August 15, 2012
Published online: September13, 2012

REFERENCES

Azuara, V., Perry, P., Sauer, S., Spivakov, M., Jørgensen, H.F., John, R.M., Gouti, M., Casanova, M., Warnes, G., Merkenschlager, M., and Fisher, A.G. (2006). Chromatin signatures of pluripotent cell lines. Nat. Cell Biol. *8*, 532–538.

Bannister, A.J., Schneider, R., Myers, F.A., Thorne, A.W., Crane-Robinson, C., and Kouzarides, T. (2005). Spatial distribution of di- and tri-methyl lysine 36 of histone H3 at active genes. J. Biol. Chem. *280*, 17732–17736.

Bernstein, B.E., Mikkelsen, T.S., Xie, X., Kamal, M., Huebert, D.J., Cuff, J., Fry, B., Meissner, A., Wernig, M., Plath, K., et al. (2006). A bivalent chromatin structure marks key developmental genes in embryonic stem cells. Cell *125*, 315–326.

Boyer, L.A., Plath, K., Zeitlinger, J., Brambrink, T., Medeiros, L.A., Lee, T.I., Levine, S.S., Wernig, M., Tajonar, A., Ray, M.K., et al. (2006). Polycomb complexes repress developmental regulators in murine embryonic stem cells. Nature *441*, 349–353.

Bu, L., Jiang, X., Martin-Puig, S., Caron, L., Zhu, S., Shao, Y., Roberts, D.J., Huang, P.L., Domian, I.J., and Chien, K.R. (2009). Human ISL1 heart progenitors generate diverse multipotent cardiovascular cell lineages. Nature *460*, 113–117.

Collas, P. (2010). Programming differentiation potential in mesenchymal stem cells. Epigenetics *5*, 476–482.

Cui, K., Zang, C., Roh, T.Y., Schones, D.E., Childs, R.W., Peng, W., and Zhao, K. (2009). Chromatin signatures in multipotent human hematopoietic stem cells indicate the fate of bivalent genes during differentiation. Cell Stem Cell *4*, 80–93.

Dahl, J.A., Reiner, A.H., Klungland, A., Wakayama, T., and Collas, P. (2010). Histone H3 lysine 27 methylation asymmetry on developmentally-regulated promoters distinguish the first two lineages in mouse preimplantation embryos. PLoS ONE *5*, e9150.

Domian, I.J., Chiravuri, M., van der Meer, P., Feinberg, A.W., Shi, X., Shao, Y., Wu, S.M., Parker, K.K., and Chien, K.R. (2009). Generation of functional ventricular heart muscle from mouse ventricular progenitor cells. Science *326*, 426–429.

Glickman, N.S., and Yelon, D. (2002). Cardiac development in zebrafish: coordination of form and function. Semin. Cell Dev. Biol. *13*, 507–513.

Guenther, M.G., Levine, S.S., Boyer, L.A., Jaenisch, R., and Young, R.A. (2007). A chromatin landmark and transcription initiation at most promoters in human cells. Cell *130*, 77–88.

Guenther, M.G., Frampton, G.M., Soldner, F., Hockemeyer, D., Mitalipova, M., Jaenisch, R., and Young, R.A. (2010). Chromatin structure and gene expression programs of human embryonic and induced pluripotent stem cells. Cell Stem Cell *7*, 249–257.

Hawkins, R.D., Hon, G.C., Lee, L.K., Ngo, Q., Lister, R., Pelizzola, M., Edsall, L.E., Kuan, S., Luu, Y., Klugman, S., et al. (2010). Distinct epigenomic landscapes of pluripotent and lineage-committed human cells. Cell Stem Cell *6*, 479–491.

Higashijima, S., Okamoto, H., Ueno, N., Hotta, Y., and Eguchi, G. (1997). High-frequency generation of transgenic zebrafish which reliably express GFP in whole muscles or the whole body by using promoters of zebrafish origin. Dev. Biol. *192*, 289–299.

James, R.G., Biechele, T.L., Conrad, W.H., Camp, N.D., Fass, D.M., Major, M.B., Sommer, K., Yi, X., Roberts, B.S., Cleary, M.A., et al. (2009). Bruton's tyrosine kinase revealed as a negative regulator of Wnt-beta-catenin signaling. Sci. Signal. *2*, ra25.

Kattman, S.J., Huber, T.L., and Keller, G.M. (2006). Multipotent flk-1+ cardiovascular progenitor cells give rise to the cardiomyocyte, endothelial, and vascular smooth muscle lineages. Dev. Cell *11*, 723–732.

Kattman, S.J., Witty, A.D., Gagliardi, M., Dubois, N.C., Niapour, M., Hotta, A., Ellis, J., and Keller, G. (2011). Stage-specific optimization of activin/nodal and BMP signaling promotes cardiac differentiation of mouse and human pluripotent stem cell lines. Cell Stem Cell *8*, 228–240.

Laflamme, M.A., Chen, K.Y., Naumova, A.V., Muskheli, V., Fugate, J.A., Dupras, S.K., Reinecke, H., Xu, C., Hassanipour, M., Police, S., et al. (2007). Cardiomyocytes derived from human embryonic stem cells in pro-survival factors enhance function of infarcted rat hearts. Nat. Biotechnol. *25*, 1015–1024.

Lee, T.I., Jenner, R.G., Boyer, L.A., Guenther, M.G., Levine, S.S., Kumar, R.M., Chevalier, B., Johnstone, S.E., Cole, M.F., Isono, K., et al. (2006). Control of developmental regulators by Polycomb in human embryonic stem cells. Cell *125*, 301–313.

Lee, H., Shamy, G.A., Elkabetz, Y., Schofield, C.M., Harrsion, N.L., Panagiotakos, G., Socci, N.D., Tabar, V., and Studer, L. (2007). Directed differentiation and transplantation of human embryonic stem cell-derived motoneurons. Stem Cells *25*, 1931–1939.

Li, B., Carey, M., and Workman, J.L. (2007). The role of chromatin during transcription. Cell *128*, 707–719.

Lindeman, L.C., Winata, C.L., Aanes, H., Mathavan, S., Alestrom, P., and Collas, P. (2010). Chromatin states of developmentally-regulated genes revealed by DNA and histone methylation patterns in zebrafish embryos. Int. J. Dev. Biol. *54*, 803–813.

Maves, L., Tyler, A., Moens, C.B., and Tapscott, S.J. (2009). Pbx acts with Hand2 in early myocardial differentiation. Dev. Biol. *333*, 409–418.

Mazzarella, L., Jørgensen, H.F., Soza-Ried, J., Terry, A.V., Pearson, S., Lacaud, G., Kouskoff, V., Merkenschlager, M., and Fisher, A.G. (2011a). Embryonic stem cell-derived hemangioblasts remain epigenetically plastic and require PRC1 to prevent neural gene expression. Blood *117*, 83–87.

Mazzarella, L., Jørgensen, H.F., Soza-Ried, J., Terry, A.V., Pearson, S., Lacaud, G., Kouskoff, V., Merkenschlager, M., and Fisher, A.G. (2011b). Embryonic stem cell-derived hemangioblasts remain epigenetically plastic and require PRC1 to prevent neural gene expression. Blood *117*, 83–87.

Mikkelsen, T.S., Ku, M., Jaffe, D.B., Issac, B., Lieberman, E., Giannoukos, G., Alvarez, P., Brockman, W., Kim, T.K., Koche, R.P., et al. (2007). Genome-wide maps of chromatin state in pluripotent and lineage-committed cells. Nature *448*, 553–560.

Minehata, K., Kawahara, A., and Suzuki, T. (2008). meis1 regulates the development of endothelial cells in zebrafish. Biochem. Biophys. Res. Commun. *374*, 647–652.

Möbius, W., and Gerland, U. (2010). Quantitative test of the barrier nucleosome model for statistical positioning of nucleosomes up- and downstream of transcription start sites. PLoS Comput. Biol. *6*, 6.

Mohn, F., Weber, M., Rebhan, M., Roloff, T.C., Richter, J., Stadler, M.B., Bibel, M., and Schübeler, D. (2008a). Lineage-specific polycomb targets and de novo DNA methylation define restriction and potential of neuronal progenitors. Mol. Cell *30*, 755–766.

Mohn, F., Weber, M., Rebhan, M., Roloff, T.C., Richter, J., Stadler, M.B., Bibel, M., and Schübeler, D. (2008b). Lineage-specific polycomb targets and de novo DNA methylation define restriction and potential of neuronal progenitors. Mol. Cell *30*, 755–766.

Murry, C.E., and Keller, G. (2008). Differentiation of embryonic stem cells to clinically relevant populations: lessons from embryonic development. Cell *132*, 661–680.

Pan, G., Tian, S., Nie, J., Yang, C., Ruotti, V., Wei, H., Jonsdottir, G.A., Stewart, R., and Thomson, J.A. (2007). Whole-genome analysis of histone H3 lysine 4 and lysine 27 methylation in human embryonic stem cells. Cell Stem Cell *1*, 299–312.

Phillips, B.W., Hentze, H., Rust, W.L., Chen, Q.P., Chipperfield, H., Tan, E.K., Abraham, S., Sadasivam, A., Soong, P.L., Wang, S.T., et al. (2007). Directed differentiation of human embryonic stem cells into the pancreatic endocrine lineage. Stem Cells Dev. *16*, 561–578.

Pjanic, M., Pjanic, P., Schmid, C., Ambrosini, G., Gaussin, A., Plasari, G., Mazza, C., Bucher, P., and Mermod, N. (2011). Nuclear factor I revealed as family of promoter binding transcription activators. BMC Genomics *12*, 181.

Rada-Iglesias, A., and Wysocka, J. (2011). Epigenomics of human embryonic stem cells and induced pluripotent stem cells: insights into pluripotency and implications for disease. Genome Med *3*, 36.

Ringrose, L., and Paro, R. (2004). Epigenetic regulation of cellular memory by the Polycomb and Trithorax group proteins. Annu. Rev. Genet. *38*, 413–443.

Schuettengruber, B., Chourrout, D., Vervoort, M., Leblanc, B., and Cavalli, G. (2007). Genome regulation by polycomb and trithorax proteins. Cell *128*, 735–745.

Simon, J.A., and Kingston, R.E. (2009). Mechanisms of polycomb gene silencing: knowns and unknowns. Nat. Rev. Mol. Cell Biol. *10*, 697–708.

Stankunas, K., Shang, C., Twu, K.Y., Kao, S.C., Jenkins, N.A., Copeland, N.G., Sanyal, M., Selleri, L., Cleary, M.L., and Chang, C.P. (2008). Pbx/Meis deficiencies demonstrate multigenetic origins of congenital heart disease. Circ. Res. *103*, 702–709.

Takeuchi, J.K., Ohgi, M., Koshiba-Takeuchi, K., Shiratori, H., Sakaki, I., Ogura, K., Saijoh, Y., and Ogura, T. (2003). Tbx5 specifies the left/right ventricles and ventricular septum position during cardiogenesis. Development *130*, 5953–5964.

Talbot, J.C., Johnson, S.L., and Kimmel, C.B. (2010). hand2 and Dlx genes specify dorsal, intermediate and ventral domains within zebrafish pharyngeal arches. Development *137*, 2507–2517.

Vakoc, C.R., Sachdeva, M.M., Wang, H., and Blobel, G.A. (2006). Profile of histone lysine methylation across transcribed mammalian chromatin. Mol. Cell. Biol. *26*, 9185–9195.

Vastenhouw, N.L., Zhang, Y., Woods, I.G., Imam, F., Regev, A., Liu, X.S., Rinn, J., and Schier, A.F. (2010). Chromatin signature of embryonic pluripotency is established during genome activation. Nature *464*, 922–926.

Yang, L., Soonpaa, M.H., Adler, E.D., Roepke, T.K., Kattman, S.J., Kennedy, M., Henckaerts, E., Bonham, K., Abbott, G.W., Linden, R.M., et al. (2008). Human cardiovascular progenitor cells develop from a KDR+ embryonic-stem-cell-derived population. Nature *453*, 524–528.

Yelon, D., Horne, S.A., and Stainier, D.Y. (1999). Restricted expression of cardiac myosin genes reveals regulated aspects of heart tube assembly in zebrafish. Dev. Biol. *214*, 23–37.

Zerucha, T., and Prince, V.E. (2001). Cloning and developmental expression of a zebrafish meis2 homeobox gene. Mech. Dev. *102*, 247–250.

Cell

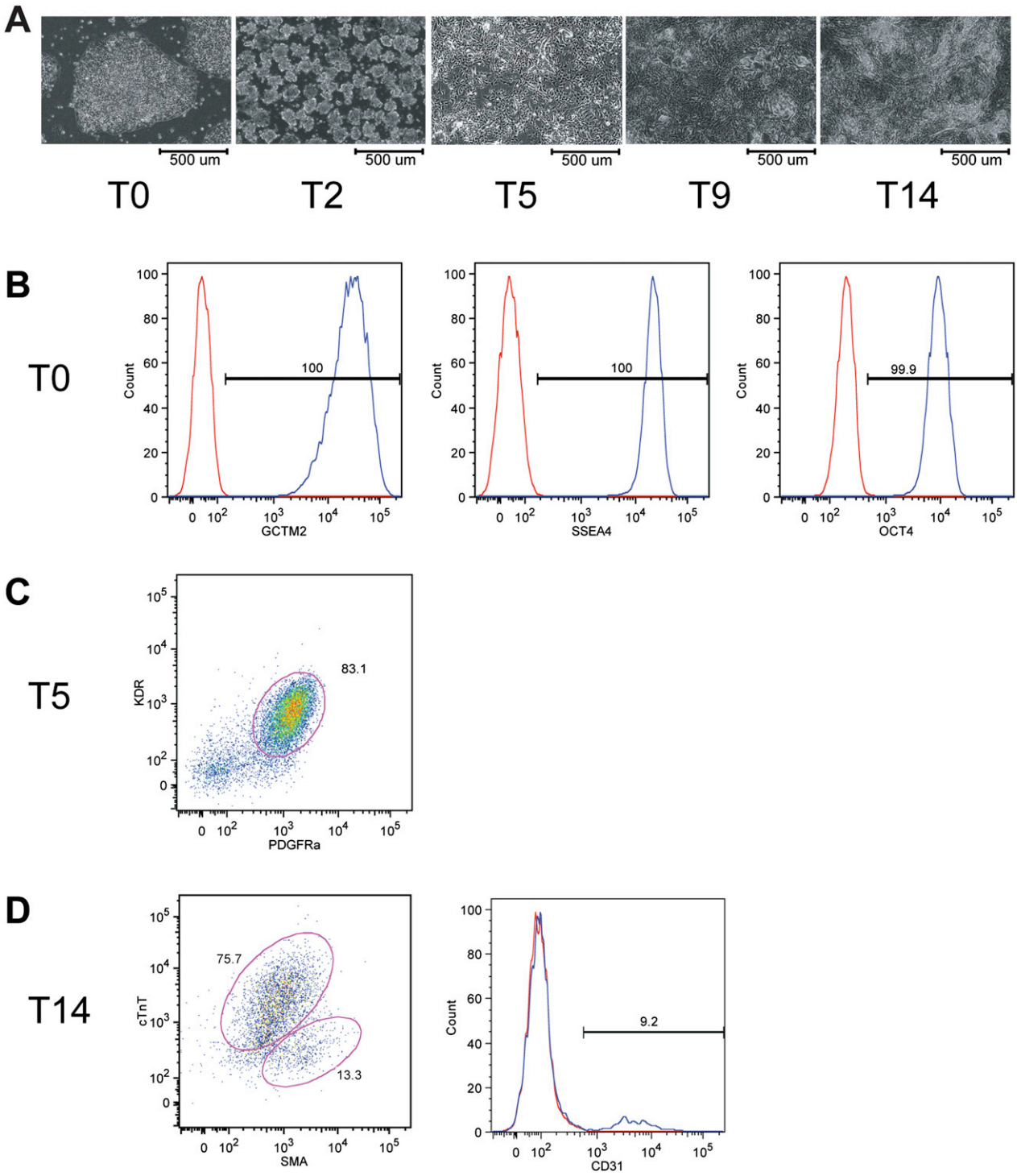

Figure S1. Cardiovascular Differentiation from Human Embryonic Stem Cells, Related to Figure 1

(A) H7 human ESCs were subjected to cardiovascular directed differentiation as described in methods. Shown are light micrograph images of the cells at the five time points used for RNA expression and ChIP-seq analysis. T0 = pluripotent hESCs; T2 = mesoderm specified cells in embryoid bodies; T5 = tripotential cardiovascular progenitors; T9 = cardiac committed; T14 = definitive cardiovascular cells.

(B) Quantification of T0 hESCs for the pluripotency markers GCTM2, SSEA4 and OCT4.

(C) Quantification of T5 tripotential cardiovascular progenitors using flow cytometry for KDR and PDGFRa.

(D) Quantification of terminal differentiation using cTnT, SMA and CD31. Cells positive for cTnT are cardiomyocytes while cells positive for SMA but negative for cTnT are smooth muscle cells. Cells expressing CD31 are endothelial cells.

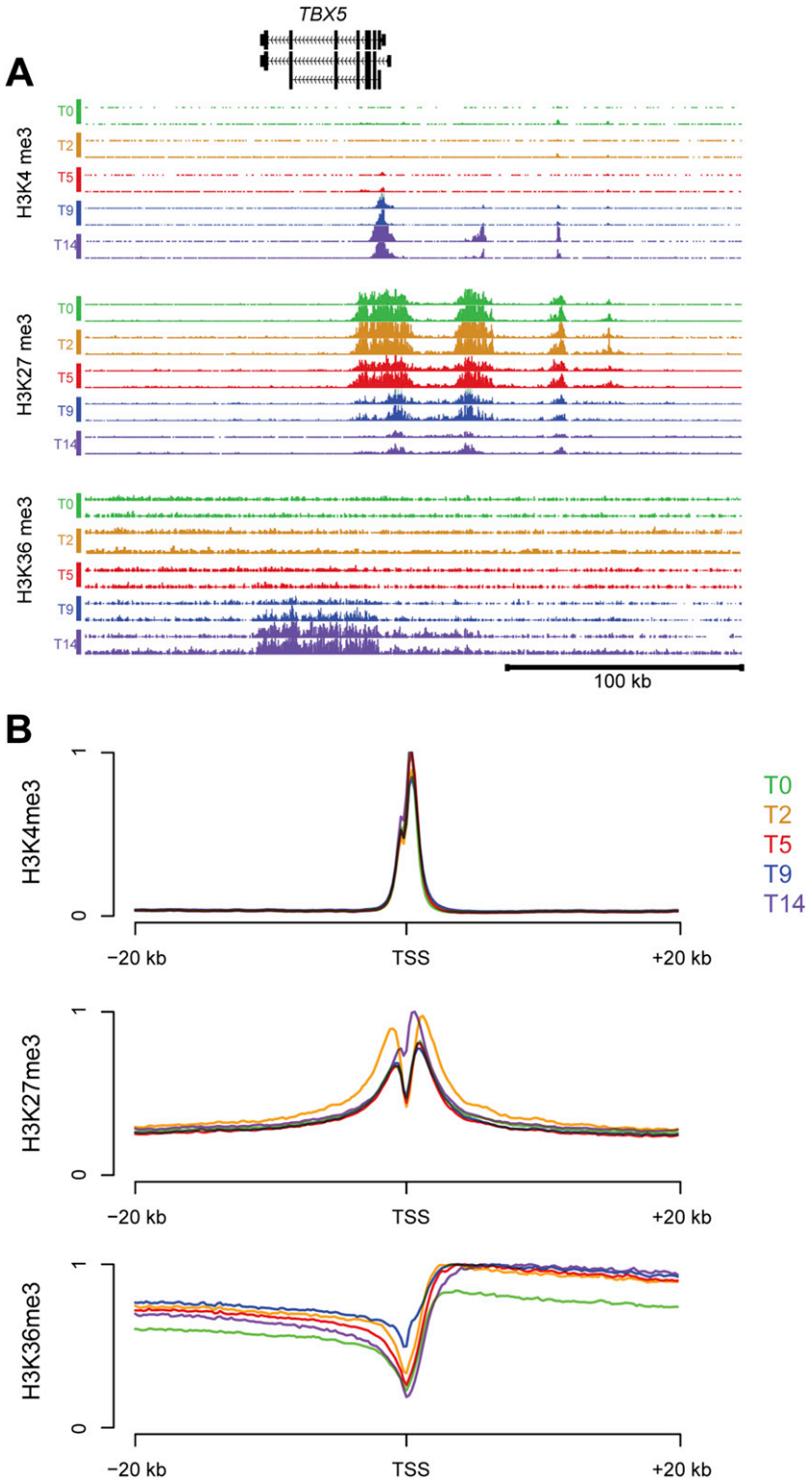

Figure S2. ChIP-seq During Cardiovascular Directed Differentiation, Related to Figure 1

(A) View of H3K4me3 (1–100), H3K27me3 (1–100) and H3K36me3 (1–25) density tracks from the UCSC genome browser at the *TBX5* locus. Shown are two replicates for each time point: T0 (pluripotent), T2 (mesoderm), T5 (tripotential cardiovascular progenitor), T9 (cardiovascular lineage committed) and T14 (definitive cardiovascular cells).

(B) Distribution of H3K4me3, H3K27me3 and H3K36me3 peaks within 20kb of annotated transcription start sites (TSS) at all five time points.

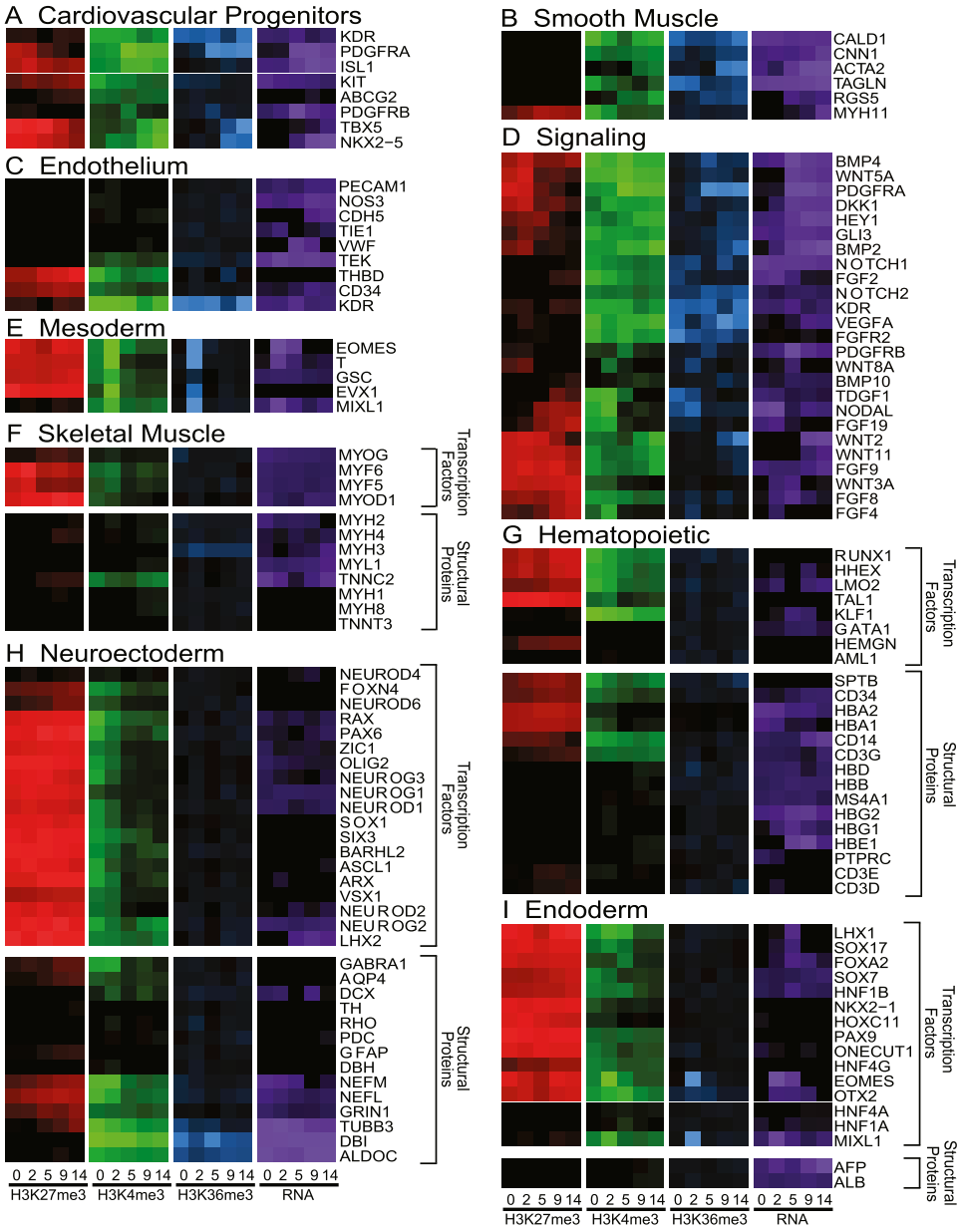

Figure S3. Histone Modification and RNA Expression Patterns for Genes Expressed in Different Cell Types, Related to Figure 1

(A–I) Patterns are shown for: (A) genes expressed in cardiovascular progenitors, (B) genes expressed in smooth muscle cells, (C) genes expressed in endothelium, (D) signaling pathway molecules involved in cardiovascular development, (E) genes involved in mesoderm specification, (F) genes expressed in skeletal muscle, (G) genes expressed in hematopoietic cells, (H) genes involved in neuroectoderm specification and differentiation or function of neuroectoderm derivatives, and (I), genes involved in endoderm specification and differentiation or function of endoderm derivatives. Format is identical to Figures 1C and 1D showing the same data for genes involved in cardiac function.

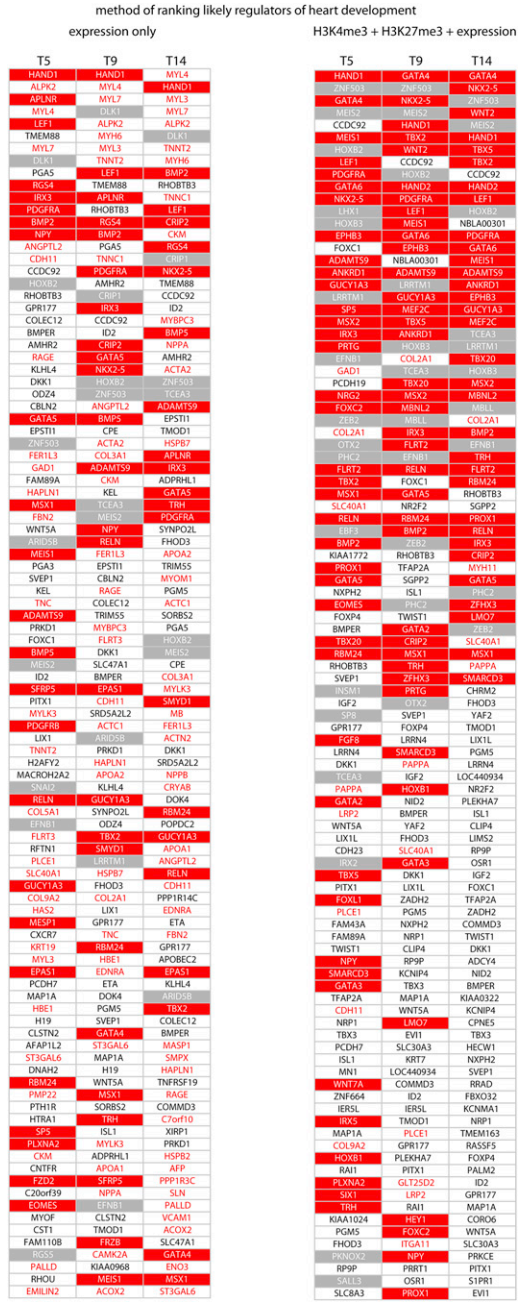

Figure S4. Classification of Genes Based on Temporal Chromatin Signature, Related to Figure 2

All genes were ranked by two different methods in order to identify key regulators of cardiac differentiation. They were ranked at days 5, 9 and 14 by a formula using either (left) RNA expression alone, or (right) one that accounts for levels of H3K4me3, H3K27me3 and RNA expression. At each time point the top 100 candidate regulators are depicted for the respective methods. Developmental regulators with known roles in cardiac differentiation are shown in white text on red background, developmental regulators with no currently-appreciated role in cardiac differentiation are shown in white text on gray background, and genes whose function pertains to the structure and function of heart cells with no known regulatory roles are shown in red text on white background. All other genes are shown in black text on white background. The top 10 from this figure are displayed in Figure 2.

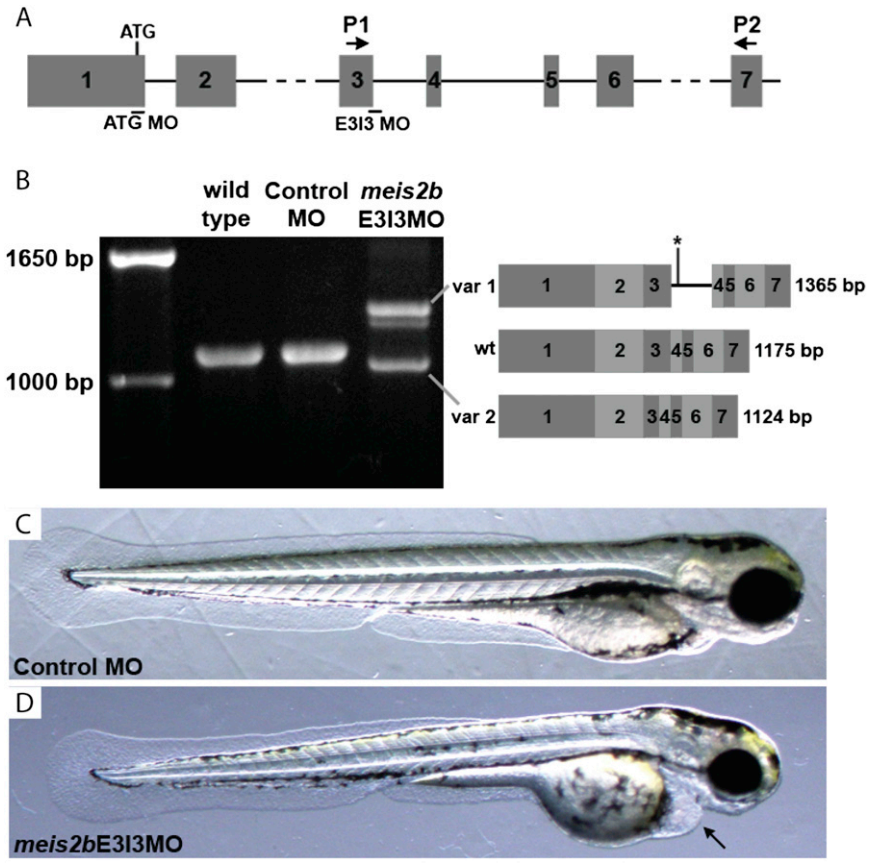

Figure S5. Validation of an Antisense Morpholino for Zebrafish *meis2b* Knockdown Shown in Figure 5

(A) Diagram of the first seven exons of zebrafish *meis2b* (NM_130910.1), shown approximately to scale, except for introns 2 and 6. Shown are the locations of binding sites for two antisense *meis2b* morpholinos, one targeting the start codon (ATG MO) to block translation, and one targeting the splice donor site for intron 3 (E3I3 MO) to block mRNA processing. Also shown are the locations of the primers (P1, P2) used in (B).

(B) Reverse transcriptase polymerase chain reaction (RT-PCR) analysis of meis2b mRNA structure in wild-type, Standard control MO (control MO), and *meis2b*E3I3MO embryos. Sequencing of these RT-PCR products revealed wild-type and control MO embryos express wild-type *meis2b* transcript, while *meis2b*E3I3MO embryos express two transcript variants (diagrammed on the right). Variant 1 (var 1) retains intron 3, which encodes a premature stop codon (*) that occurs upstream of the Meis2b homeodomain. Variant 2 (var 2) results from aberrant splicing to an upstream cryptic splice donor, resulting in the loss of 51 base pairs of exon 3 but maintenance of the correct open reading frame in exon 4.

(C and D) Live 72 hpf control MO and *meis2b*E3I3MO embryos. *meis2b*E3I3MO embryos show mild pericardial edema (arrow), as well as variable smaller heads and body curvature phenotypes. Anterior is to the right.